Self-consistent relativistic calculation of nucleon mean free path

G. Q. Li* and R. Machleidt
Department of Physics, University of Idaho, Moscow, Idaho 83843

Y. Z. Zhuo
China Institute of Atomic Energy, P.O. Box 275, Beijing, China
and Institute of Theoretical Physics, P.O. Box 2735, Beijing, China
(Received 30 March 1993)

We present a fully self-consistent and relativistic calculation of the nucleon mean free path in nuclear matter and finite nuclei. Starting from the Bonn potential, the Dirac-Brueckner-Hartree-Fock results for nuclear matter are parametrized in terms of an effective σ-ω Lagrangian suitable for the relativistic density-dependent Hartree-Fock (RDHF) approximation. The nucleon mean free path in nuclear matter is derived from this effective Lagrangian taking diagrams up to fourth-order into account. For the nucleon mean free path in finite nuclei, we make use of the density determined by the RDHF calculation in the local density approximation. Our microscopic results are in good agreement with the empirical data and predictions by Dirac phenomenology.

PACS number(s): 21.65.+f

I. INTRODUCTION

One important quantity of a medium is the mean free path of its elementary constituents. In nuclear physics, the nucleon mean free path is of special importance since it can be large compared to the nuclear size such that the basic assumption of the independent particle motion of the shell model is reasonable [1]. In nuclear reactions, the nucleon mean free path is a useful concept for summarizing a large number of experimental data [2,3]. Furthermore, in the investigation of heavy-ion reactions, the mean free path of nucleons and other hadrons are often used to estimate the number of two-body collisions and the reabsorption effect of the medium on the production cross sections of hadrons [4].

Most calculations of the nucleon mean free path have been done in the framework of nonrelativistic dynamics [5–11], based on, e.g., the phenomenological Skyrme force. Characteristic for the early theoretical investigations [5,6] is the underestimation of the nucleon mean free path by up to a factor of two as compared to the empirical value. The proper treatment of the nonlocality of the nucleon optical potential resolves much of the discrepancy between the theoretical prediction and the empirical data [7,9]. The nonlocality of the nucleon optical potential (or mean field) leads to the reduction of the nucleon mass and consequently increases the nucleon mean free path, which is known as the Negele-Yazaki enhancement [7].

Recently there have been some relativistic calculations of the nucleon mean free path [12–15], based on either Dirac phenomenology or the relativistic impulse approximation for the nucleon optical potential. In this paper, we present a fully self-consistent and relativistic calculation of the nucleon mean free path in nuclear matter, starting from the Bonn potential as the realistic nucleon-nucleon (NN) interaction. The nucleon self-energy (optical potential) is derived from the Dirac-Brueckner-Hartree-Fock (DBHF) results for nuclear matter, which includes the important medium effects.

This work is a continuation of our effort [16–19] to describe self-consistently the properties of nuclear matter, finite nuclei, and nuclear reactions based on the same realistic NN interaction. There are two aspects to this problem. First, one needs a realistic NN interaction which is ultimately determined by the underlying dynamics of quarks and gluons and should in principle be derived from quantum chromodynamics (QCD). However, due to the nonperturbative character of QCD in the low-energy regime relevant for nuclear physics, we are far away from a quantitative understanding of the NN interaction in this way. On the other hand, there is a good chance that conventional hadrons, like nucleons and mesons, remain the relevant degrees of freedom for a wide range of nuclear physics phenomena. In that case, the overwhelming part of the NN potential can be constructed in terms of meson-baryon interactions. In fact, the only quantitative NN interactions available up until now are based on meson exchange; a well-known example is the Bonn potential [16,20] which we apply in this work.

The second aspect of the problem concerns a suitable many-body theory that is able to deal with the bare NN interaction which has a strong repulsive core. The Brueckner approach [21–23] and the variational method [24,25] have been developed for this purpose. However, when using two-body forces, both many-body theories are not able to reproduce correctly the saturation properties of nuclear matter. Inspired by the success

*Present address: Cyclotron Institute, Texas A&M University, College Station, TX 77843.

of Dirac phenomenology in intermediate-energy proton-nucleus scattering [26,27] and the Walecka model (QHD) for dense nuclear matter [28,29], a relativistic extension of the Brueckner approach has been initiated by Shakin and co-workers [30], frequently called the Dirac-Brueckner-Hartree-Fock (DBHF) approach. This approach has been further developed by Brockmann and Machleidt [16,17] and by ter Haar and Malfliet [31]. The common feature of all DBHF results is that a repulsive relativistic many-body effect is obtained which is strongly density dependent such that the empirical nuclear matter saturation can be explained. The Bonn potential and the DBHF approach thus provide a reasonable starting point for pursuing the longstanding goal of self-consistently describing nuclear matter, finite nuclei and nuclear reactions based on the same realistic NN interaction.

In order to carry out a systematic self-consistent study of nuclear properties, one usually parametrizes the DBHF results for nuclear matter in terms of an effective Lagrangian, which, in relativistic density-dependent Hartree Fock (RDHF) approximation, leads to the same predictions for nuclear matter as the original DBHF calculation. The effective Lagrangian, with its parameters determined by the underlying NN interaction, can then be used in other domains of nuclear physics, e.g., the structure of finite nuclei and nuclear reactions. Different schemes for this parametrization have been proposed [32–35]. We use in the present work the scheme recently suggested by Brockmann and Toki [34] in which the DBHF results for nuclear matter with the Bonn potential are parametrized in terms of an effective σ-ω Lagrangian. This scheme is however extended to the relativistic density-dependent Hartree-Fock (RDHF) approximation, which is more appropriate than the relativistic density-dependent Hartree (RDH) approximation of Ref. [34]. The coupling constants of these effective mesons are density dependent, and are determined from the underlying bare NN interaction via a DBHF calculation. The nucleon self-energy (optical potential), and hence the nucleon mean free path, are then calculated based on this effective Lagrangian up to the fourth-order Feynman diagrams. For the calculation of the nucleon self-energy and mean free path in finite nuclei, we use the nucleon density determined by the RDHF calculation [36] in the local density approximation.

We outline the formalism of this work in Sec. II. The results and discussion are presented in Sec. III. The paper ends with a brief summary in Sec. IV.

II. FORMALISM

The relativistic Bonn potential to be used in this work is constructed in terms of the Thompson equation which is a three-dimensional reduction to the original Bethe-Salpeter equation. The kernel of the Thompson equation, $V(\mathbf{q}', \mathbf{q})$, is the sum of one-meson-exchange amplitudes of certain bosons with given mass and coupling. In the one-boson-exchange (OBE) Bonn model [16], six nonstrange bosons with mass below 1 GeV are used. Three sets of potential parameters, denoted by Bonn A, B, and C, have been proposed (and are given in Table A.2 of Ref. [16]). The main difference between the three parameter sets is the cutoff mass for the πNN vertex, which is 1.05, 1.2, and 1.3 GeV for Bonn A, B, and C, respectively. Consequently, the three potentials differ in the strength of their tensor force component; Bonn A has the weakest tensor force. All three potentials reproduce the deuteron properties and the phase shifts of NN scattering accurately (cf. Refs. [16,17]).

The Bonn potential is used in the DBHF calculation for nuclear matter. The essential point of this approach is the use of the Dirac equation for the description of the single-particle motion in the nuclear medium

$$[\boldsymbol{\alpha}\cdot\mathbf{k} + \beta(m + U_S) + U_V^0]\tilde{u}(\mathbf{k}, s) = E\tilde{u}(\mathbf{k}, s) \tag{1}$$

where U_S is an attractive scalar field and U_V^0 is (the time-like component of) a repulsive vector field.

As in conventional Brueckner theory, the basic quantity in the DBHF approach is the $\tilde{G}$-matrix which satisfies the in-medium Thompson equation (also known as relativistic Bethe-Goldstone equation) [16,17,19]

$$\tilde{G}(\mathbf{q}', \mathbf{q}|\mathbf{P}, \tilde{z}) = \tilde{V}(\mathbf{q}', \mathbf{q}) + \int \frac{d^3k}{(2\pi)^3} \tilde{V}(\mathbf{q}', \mathbf{k}) \frac{\tilde{m}^2}{\tilde{E}^2_{(1/2)\mathbf{P}+\mathbf{k}}} \frac{Q(\mathbf{k}, \mathbf{P})}{2\tilde{E}_{(1/2)\mathbf{P}+\mathbf{q}} - 2\tilde{E}_{(1/2)\mathbf{P}+\mathbf{k}}} \tilde{G}(\mathbf{k}, \mathbf{q}|\mathbf{P}, \tilde{z}) \tag{2}$$

with

$$\tilde{m} = m + U_S \text{ and } \tilde{E}_{\mathbf{k}} = (\mathbf{k}^2 + \tilde{m}^2)^{(1/2)}$$

and $\mathbf{P}$ the c.m. momentum of the two colliding nucleons in the nuclear medium.

Since the kernel of the in-medium Thompson equation depends on the solution of the Dirac equation, while the Dirac equation needs the scalar and vector potentials which are determined from the $\tilde{G}$ matrix, one is dealing with a self-consistency problem [16,17]. The nuclear matter properties are then obtained from the in-medium two-body interaction, the $\tilde{G}$ matrix. Applying the Bonn A potential, the DBHF calculation predicts that nuclear matter saturates at 0.185 fm^{-3} with an energy per nucleon $\mathcal{E}/A$=−15.6 MeV, which is in good agreement with the empirical values. More results and discussions concerning the properties of nuclear matter as predicted by the DBHF approach can be found in Refs. [16,17,19].

As proposed by Brockmann and Toki [34], the DBHF results for nuclear matter can be parametrized by an effective Lagrangian, in analogy to the σ-ω model of Walecka:

$$\mathcal{L} = \bar{\psi}[i\gamma_\mu\partial^\mu - m - g_\sigma(\rho)\phi_\sigma - g_\omega(\rho)\gamma_\mu\phi_\omega^\mu]\psi + \frac{1}{2}(\partial^\mu\phi_\sigma)^2 - \frac{1}{2}m_\sigma^2\phi_\sigma^2 - \frac{1}{4}(\partial_\mu\phi_\omega^\nu - \partial_\nu\phi_\omega^\mu)^2 + \frac{1}{2}m_\omega^2\phi_\omega^{\mu 2} \quad (3)$$

where ψ is the nucleon field, while ϕ_σ and ϕ_ω^μ are the effective sigma and omega fields, respectively. The masses of the effective sigma and omega mesons are kept fixed at their values in free-space scattering. However, the density-dependent coupling constants are choosen such as to reproduce the DBHF results for nuclear matter when Eq. (3) is applied in the RDHF approximation.

Treating the effective coupling constants locally as numbers and calculating in the RDHF approximation, the nucleon self-energy can be expressed as

$$\Sigma(k_\mu) = \Sigma_S(k_\mu) + \gamma^0\Sigma_0(k_\mu) + \boldsymbol{\gamma}\cdot\mathbf{k}\Sigma_V(k_\mu) \quad (4)$$

where Σ_S, Σ_0, and Σ_V denotes the scalar component, the timelike part of the vector component and the spacelike part of the vector component of the nucleon self-energy, respectively. Explicitly the real part of the nucleon self-energy is given by [29,37]

$$\Sigma_S(\rho,k) = -\frac{2}{\pi^2}\frac{g_\sigma^2(\rho)}{m_\sigma^2}\int_0^{k_F} dqq^2\frac{m_q^*}{E_q^*} + \frac{1}{16\pi^2 k}\int_0^{k_F} dqq\frac{m_q^*}{E_q^*}[g_\sigma^2(\rho)\Theta_\sigma(k,q) - 4g_\omega^2(\rho)\Theta_\omega(k,q)], \quad (5)$$

$$\Sigma_0(\rho,k) = \frac{2}{\pi^2}\frac{g_\omega^2(\rho)}{m_\omega^2}\int_0^{k_F} dqq^2 + \frac{1}{16\pi^2 k}\int_0^{k_F} dqq[g_\sigma^2(\rho)\Theta_\sigma(k,q) + 2g_\omega^2(\rho)\Theta_\omega(k,q)], \quad (6)$$

$$\Sigma_V(\rho,k) = -\frac{1}{8\pi^2 k^2}\int_0^{k_F} dqq\frac{q^*}{E_q^*}[g_\sigma^2(\rho)\Phi_\sigma(k,q) + 2g_\omega^2(\rho)\Phi_\omega(k,q)] \quad (7)$$

where

$$\Theta_i(k,q) = \ln\left|\frac{A_i(k,q)+2kq}{A_i(k,q)-2kq}\right|,$$

$$\Phi_i(k,q) = \frac{A_i(k,q)\Theta_i(k,q)}{4kq} - 1,$$

$$A_i(k,q) = \mathbf{k}^2 + \mathbf{q}^2 + m_i^2 - (q_0 - k_0)^2, \quad i = \sigma,\omega$$

and

$$m_k^* = m + \Sigma_S(\rho,k), \quad (8)$$

$$\mathbf{k}^* = \mathbf{k}(1 + \Sigma_V(\rho,k)), \quad (9)$$

$$k_0 = (\mathbf{k}^{*2} + m_k^{*2})^{1/2} + \Sigma_0. \quad (10)$$

In determining the effective coupling constants from these expressions, we drop the spacelike component of the vector potential and calculate at the Fermi surface, by identifying Σ_S and Σ_0 with U_S and U_0^0 obtained in the DBHF calculation. This is a reasonable assumption since the spacelike component is very small and the potentials are only very weakly momentum dependent.

There are mainly two differences between our effective Lagrangian, Eq. (3), and the Walecka model [28,29]. First, the coupling constants in our model are no longer free parameters fitted to the nuclear matter saturation properties; these effective coupling constants are determined by the DBHF calculation in which a realistic NN interaction is used. Second, the coupling constants of our effective Lagrangian are density dependent, whereas those in the Walecka model are density independent. The absence of density dependence in the Walecka model may be responsible for its unrealistically large incompressibility.

In the RDHF approximation, the real part of the nucleon self-energy contains the energy-independent Hartree contributions [see Fig. 1(a)] as well as the energy-dependent Fock contributions [see Fig. 1(b)]. The lowest-order contribution to the imaginary part of the nucleon self-energy is the fourth-order Feynman diagram which is characterized by two-particle–one-hole ($2p1h$) intermediate states [see Fig. 1(c)]. The nucleon lines in these Feynman diagrams are described by dressed nucleon propagators, which corresponds to performing the calculation on the Hartree-Fock ground state and taking account of all Hartree-Fock insertions. The explicit expressions for the imaginary part of the nucleon self-energy have been given in Ref. [38]. The derivation of the nucleon self-energy from the Walecka model has been discussed in detail in Refs. [37,38]. For the effective Lagrangian used in the present work, the expressions for the nucleon self-energy are the same, but with the coupling constants for sigma and omega exchange replaced by the density-dependent ones as determined in the nuclear matter DBHF calculation.

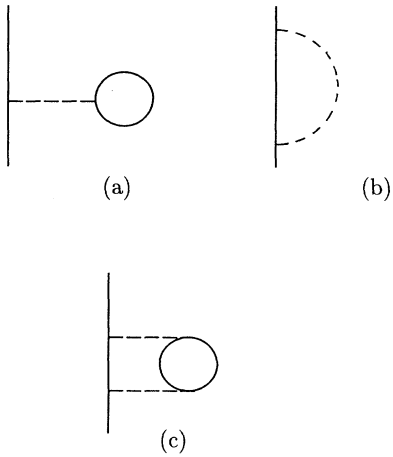

FIG. 1. Feynman diagrams for the calculation of the nucleon self-energy in nuclear matter. (a) Hartree diagram, (b) Fock diagram, (c) fourth-order diagram.

The spacelike part of the vector potential, Σ_V, is rather small compared to other terms in Eq. (4) and can be absorbed into the scalar potential and the timelike part of the vector potential by the following transformation

$$U_S = \frac{\Sigma_S - m\Sigma_V}{1+\Sigma_V}, \quad U_V = \frac{\Sigma_0 + E\Sigma_V}{1+\Sigma_V}. \tag{11}$$

In terms of the scalar potential U_S and the vector potential U_V, the momentum of a nucleon propagating through a uniform nuclear medium can be determined from

$$E = [(m+U_S)^2 + k^2]^{1/2} + U_V. \tag{12}$$

This can be rewritten as

$$\frac{k^2}{2m} + V + iW = E - m + \frac{(E-m)^2}{2m} \tag{13}$$

with

$$V = U_{SR} + U_{VR} + \frac{(E-m)}{m}U_{VR} + \frac{1}{2m}(U_{SR}^2 + U_{VI}^2 - U_{SI}^2 - U_{VR}^2),$$

$$W = U_{SI} + U_{VI} + \frac{(E-m)}{m}U_{VI} + \frac{1}{m}(U_{SR}U_{SI} - U_{VR}U_{VI})$$

where we distinguish between the real and imaginary part of the scalar and vector potential given by

$$U_S = U_{SR} + iU_{SI},$$

$$U_V = U_{VR} + iU_{VI}$$

Since $(V+iW)$ can be identified as the Schrödinger equivalent potential which is the nucleon optical potential in the non-relativistic approach, Eq. (13) is identical to the non-relativistic dispersion relation, except for the relativistic correction, $(E-m)^2/2m$.

Since the potentials U_S and U_V are complex, the nucleon momentum is also complex and can be expressed as

$$k = k_R + ik_I. \tag{14}$$

The nucleon mean free path, λ, is related to the imaginary part of the nucleon momentum by [7]

$$\lambda = \frac{1}{2k_I}. \tag{15}$$

From Eqs. (13), (14) and (15) we obtain an analytical expression for the nucleon mean free path

$$\lambda = \frac{1}{2}\left\{-m\left(E - m - V + \frac{(E-m)^2}{2m}\right) + m\left[\left(E - m - V + \frac{(E-m)^2}{2m}\right)^2 + W^2\right]^{1/2}\right\}^{-1/2}. \tag{16}$$

Since empirical information on the nucleon mean free path is usually obtained by analyzing nucleon-nucleus scattering data, it is also of interest to perform a microscopic calculation of the nucleon mean free path in finite nuclei. To calculate the nucleon self-energy (optical potential) and mean free path in finite nuclei, one often makes use of the local density approximation. With this approximation, the spatial dependence of the nucleon self-energy is directly related to the density of the nucleus under consideration. Thus in addition to the expressions for the nucleon self-energy in nuclear matter, as outlined above, we also need to know the density of the finite nucleus, so that we can calculate the nucleon mean free path in finite nuclei. To attain self-consistency of our calculations, the density of the finite nucleus must be determined in a RDHF calculation with the effective Lagrangian, Eq. (3). Such a calculation has recently been carried out by Fritz *et al.* [36] for ^{40}Ca, which we use in our calculation of the nucleon mean free path. Note that in finite nuclei, the incident energy $T_{\rm lab}$ is related to the total energy E by

$$E = \frac{m^2 + m_T(m + T_{\rm lab})}{[(m+m_T)^2 + 2m_T T_{\rm lab}]^{1/2}} \tag{17}$$

where m and m_T are the masses of the nucleon and the nucleus, respectively.

III. RESULTS AND DISCUSSIONS

The coupling constants of the sigma and omega meson of the effective Lagrangian are shown in Figs. 2(a) (sigma) and 2(b) (omega). Both effective coupling constants drop with increasing density. There are some differences between the effective coupling constants derived from the Bonn A, B, and C potentials; those based on Bonn C decrease more with increasing density. This difference can be traced back to differences in the tensor-force strength of these potentials [39].

From the effective Lagrangian we derive the nucleon self-energy (optical potential) up to the fourth-order Feynman diagrams (see Fig. 1). In Fig. 3, we show the scalar and vector potential, U_S and U_V, as defined by Eqs. (4) and (11). We consider two cases with density ρ=(1/2)ρ_0 (solid curves) and ρ_0 (dashed curves); $\rho_0 = 0.17$ fm^{-3} is the density of normal nuclear matter. The results are obtained with the Bonn A potential. The incident energy $T_{\rm lab}$ is related to the total energy E by $E = T_{\rm lab} + m$. Whereas the real part of these potentials depends only weakly on the incident energy and decreases slightly (in magnitude) with increasing energy, the imaginary part depends strongly on the incident energy and increases (in magnitude) very fast with energy.

With the scalar potential U_S and the vector poten-

tial U_V derived from the effective Lagrangian, we can calculate self-consistently the nucleon mean free path in nuclear matter starting from the bare NN interaction. No parameters beyond those of the Bonn potential are involved in the present calculation. The nucleon mean free path is calculated from Eq. (16). The results in normal nuclear matter, which simulates the interior of heavy nuclei, are shown in Fig. 4. The solid, long-dashed and short-dashed curves represent the self-consistent results based on the Bonn A, B, and C potentials, respectively, whereas the dotted curve is the result derived from the original σ-ω model of Walecka (QHD-I) [29]. The dots with error bars represent early empirical values of the nucleon mean free path extracted from experiment [40]. The shaded area indicates the estimation of the nucleon mean free path based on total reaction cross sections [3]. The solid squares correspond to the recent empirical data based on Dirac phenomenology in an energy-dependent analysis [14,15]. It is clear that there are still large ambiguities in the empirical determination of the nucleon mean free path. Within the error range involved, our results based on the Bonn potential are in reasonable agreement with the empirical data in the whole energy region considered in this work. Comparing with the latest empirical data based on Dirac phenomenology, our results are slightly larger at low energies and in agreement at high energies, whereas the results based on the

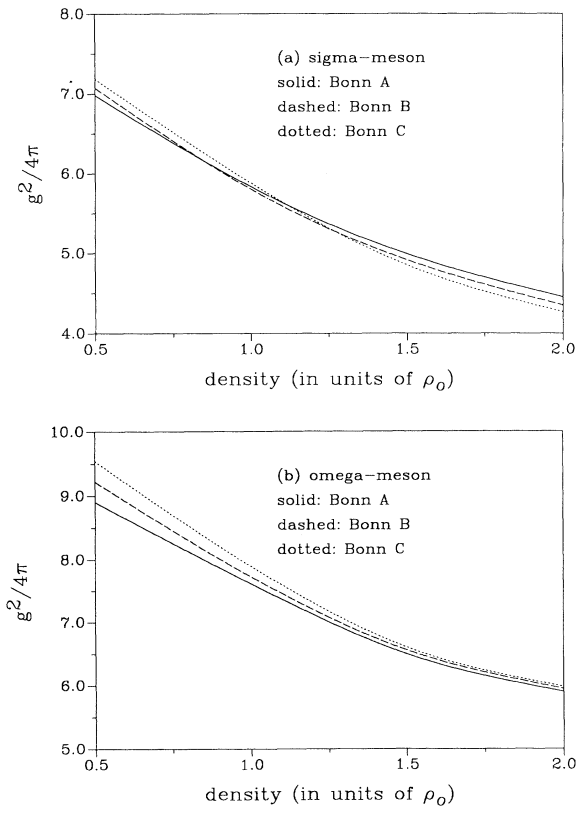

FIG. 2. Density dependence of the coupling constants for (a) sigma and (b) omega.

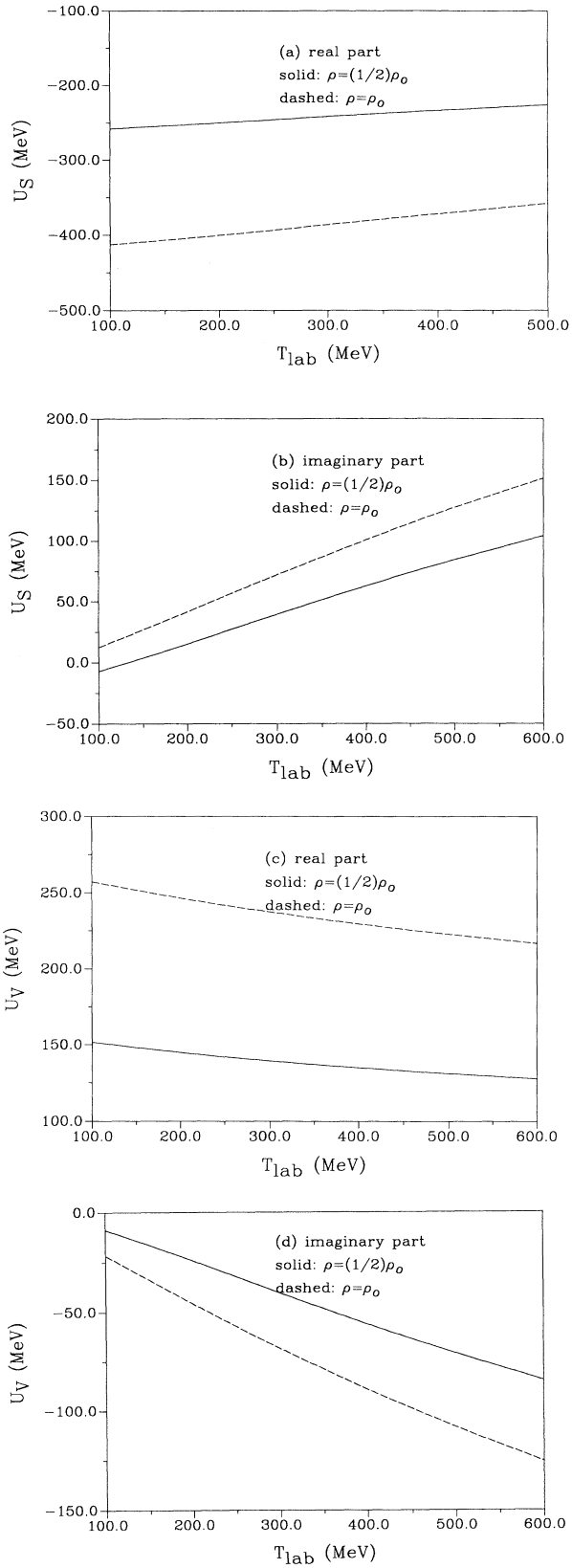

FIG. 3. Energy and density dependence of the scalar potential U_S [(a) and (b)] and vector potential U_V [(c) and (d)] in nuclear matter, using the Bonn A potential.

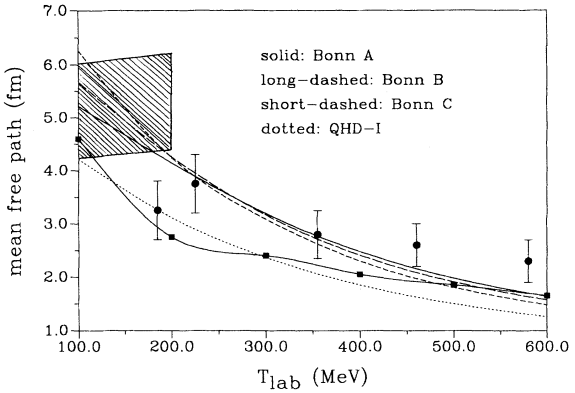

FIG. 4. Energy dependence of the nucleon mean free path in normal nuclear matter. The solid dots with error bars are from Ref. [40], the shaded area is from Ref. [3] and the solid squares from Ref. [14].

QHD-I model are in agreement at low energies and too small at higher energies. Between the self-consistent results corresponding to Bonn A, B, and C, there is also some difference which is due to the differences in the effective coupling constants (cf. Fig. 2).

Also of interest is the density dependence of the nucleon mean free path. This information is sometimes needed in the description of heavy-ion reactions where dense nuclear matter with density up to $(2–3)\rho_0$ is formed. In Fig. 5 we show the density dependence of the nucleon mean free path, corresponding to two incident energies. The results are obtained with the Bonn A potential. The mean free path decreases with the increasing density, especially at low density.

Finally we show in Fig. 6 the nucleon mean free path in ^{40}Ca as a function of the radial distance r. The solid, dashed and dotted curves correspond to nucleon energies $T_{\rm lab}$=150, 300 and 450 MeV, respectively. In the center of the nucleus, the nucleon mean free path is about 2–5 fm, depending on the energy of nucleon. The nucleon mean free path increases rapidly at the surface of the nucleus due to the decrease of the nucleon density.

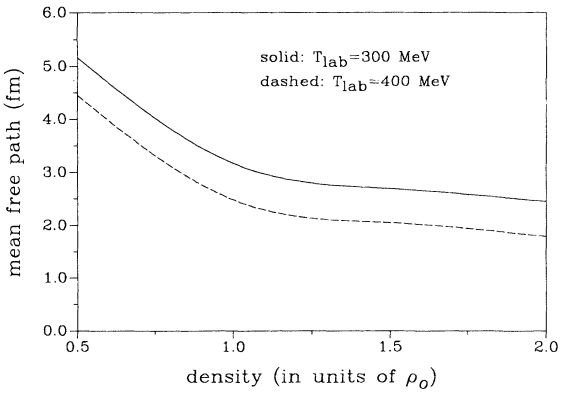

FIG. 5. Density dependence of the nucleon mean free path at two energies. Results are obtained with the Bonn A potential.

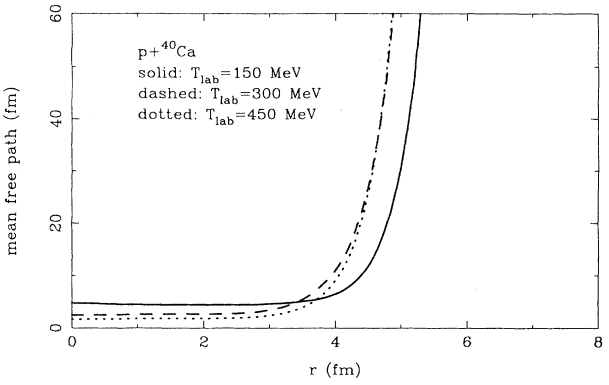

FIG. 6. Nucleon mean free path in ^{40}Ca as function of radial distance r. The solid, dashed and dotted curves correspond to $T_{\rm lab}$=150, 300, and 450 MeV, respectively. The results are obtained with the Bonn A potential.

IV. SUMMARY AND OUTLOOK

In this paper, we have presented a fully self-consistent calculation of the nucleon mean free path in nuclear matter and finite nuclei, starting from a realistic NN interaction (the Bonn potential). In order to facilitate a systematic investigation of nuclear properties, we have parametrized the DBHF results for nuclear matter in terms of an effective σ-ω Lagrangian. The density dependent coupling constants of this effective Lagrangian are determined such as to reproduce the DBHF results for nuclear matter in the RDHF approximation. The effective coupling constants decrease with increasing density.

In the derivation of the nucleon self-energy (optical potential) based on the effective Lagrangian, diagrams up to the fourth order are included. The nucleon mean free path is then calculated from the nucleon optical potential through a dispersion relation. Our results for the nucleon mean free path in nuclear matter are in good agreement with empirical data. We have also analyzed the density and energy dependence of the nucleon mean free path and find that it decreases with increasing density and energy.

We have also calculated the nucleon mean free path in finite nuclei by means of the local density approximation. For this purpose, we made use of the density of ^{40}Ca as determined in a RDHF calculation with the effective Lagrangian, Eq. (3) [36]. In the center of the nucleus, the nucleon mean free path was found to be in reasonable agreement with empirical data.

Another aspect is the temperature dependence of the nucleon mean free path, in addition to its dependence on density and energy. This is of interest for heavy-ion reactions where a piece of hot and dense nuclear matter is formed. This problem is under investigation.

ACKNOWLEDGMENT

One of the authors (G.Q.L.) thanks Professor H. Müther for the RDHF density of ^{40}Ca. This work was supported in part by the U.S. National Science Foundation under Grant No. PHY-9211607, and by the Idaho State Board of Education.

[1] A. Bohr and B. Mottleson, *Nuclear Structure* (Benjamin, New York, 1969).
[2] R. M. Devries and N. J. DiGiacomo, J. Phys. G **7**, L51 (1981).
[3] A. Nadasen *et al.*, Phys. Rev. C **23**, 1023 (1981).
[4] G. Q. Li, T. D. Khoa, T. Maruyama, S. W. Huang, N. Ohtsuka, A. Faessler, and J. Aichelin, Nucl. Phys. **A534**, 697 (1991).
[5] J. P. Schiffer, Nucl. Phys. **A335**, 348 (1980).
[6] M. T. Collins and J. J. Griffin, Nucl. Phys. **A348**, 63 (1980).
[7] J. W. Negele and K. Yazaki, Phys. Rev. Lett. **47**, 71 (1981).
[8] H. O. Meyer and P. Schwandt, Phys. Lett. **107B**, 353 (1981).
[9] S. Fantoni, B. L. Friman, and V. R. Pandharipande, Phys. Lett. **104B**, 89 (1981).
[10] A. H. Blin, R. W. Hasse, B. Hiller, and P. Schuck, Phys. Lett. **161B**, 211 (1985).
[11] G. Q. Li, J. Phys. **G17**, 1 (1991).
[12] T. Cheon, Phys. Rev. C **38**, 1516 (1988).
[13] R. A. Rego, Phys. Rev. C **44**, 1944 (1991).
[14] E. D. Cooper, S. Hama, B. C. Clark, and R. L. Mercer, Phys. Rev. C **47**, 297 (1993).
[15] B. C. Clark, E. D. Cooper, S. Hama, R. W. Finlay, and T. Adami, Phys. Lett. B **229**, 189 (1993).
[16] R. Machleidt, Adv. Nucl. Phys. **19**, 189 (1989).
[17] R. Brockmann and R. Machleidt, Phys. Rev. C **42**, 1965 (1990).
[18] H. Müther, R. Machleidt, and R. Brockmann, Phys. Rev. C **42**, 1981 (1990).
[19] G. Q. Li, R. Machleidt, and R. Brockmann, Phys. Rev. C **45**, 2782 (1992).
[20] R. Machleidt, K. Holinde, and Ch. Elster, Phys. Rep. **149**, 1 (1987).
[21] K. A. Brueckner, C. A. Levinson, and H. M. Mahmoud, Phys. Rev. **95**, 217 (1954).
[22] H. A. Bethe, Phys. Rev. **103**, 1352 (1956).
[23] J. Goldstone, Proc. R. Soc. London **A239**, 267 (1957).
[24] R. Jastrow, Phys. Rev. **98**, 1479 (1955).
[25] V. R. Pandharipande and R. B. Wiringa, Rev. Mod. Phys. **51**, 821 (1979).
[26] L. G. Arnold, B. C. Clark, R. L. Mercer, and P. Shwandt, Phys. Rev. C **19**, 917 (1979).
[27] S. J. Wallace, Annu. Rev. Nucl. Part. Sci. **37**, 267 (1987).
[28] J. D. Walecka, Ann. Phys. (N.Y.) **83**, 491 (1974).
[29] B. D. Serot and J. D. Walecka, Adv. Nucl. Phys. **16**, 1 (1986).
[30] M. R. Ansatasio, L. S. Celenza, W. S. Pong, and C. M. Shakin, Phys. Rep. **100**, 327 (1983).
[31] B. ter Haar and R. Malfliet, Phys. Rep. **149**, 207 (1987).
[32] H. Elsenhans, H. Müther, and R. Machleidt, Nucl. Phys. **A515**, 715 (1990).
[33] S. Marcos, M. Lopez-Quelle, and N. Van Giai, Phys. Lett. **B257**, 5 (1991).
[34] R. Brockmann and H. Toki, Phys. Rev. Lett. **68**, 340 (1992).
[35] S. Gmuca, Nucl. Phys. **A547**, 447 (1992).
[36] R. Fritz, H. Müther, and R. Machleidt, Phys. Rev. Lett. **71**, 46 (1993).
[37] C. J. Horowitz and B. D. Serot, Nucl. Phys. **A399**, 529 (1983).
[38] C. J. Horowitz, Nucl. Phys. **A412**, 228 (1984).
[39] R. Machleidt and G. Q. Li, invited talk presented at Realistic Nuclear Structure, a conference to mark the 60th brithday of T. T. S. Kuo, Phys. Rep. (to be published).
[40] P. U. Renberg, D. F. Measday, P. Pepin, P. Schwaller, B. Favier, and C. Richard-Serre, Nucl. Phys. **A183**, 81 (1972).